MECHANICAL TESTING
OF
WELD SIMULATED HSLA STEELS

By

MANJUL SARMA

Department of Materials & Metallurgical Engineering

INDIAN INSTITUTE OF TECHNOLOGY KANPUR

JANUARY, 1997

MECHANICAL TESTING

OF

WELD SIMULATED HSLA STEELS

A Thesis submitted
in Partial fulfilment of the Requirements
for the Degree of

MASTER OF TECHNOLOGY

by

MANJUL SARMA

Department of Materials & Metallurgical Engineering
INDIAN INSTITUTE OF TECHNOLOGY
KANPUR

CERTIFICATE

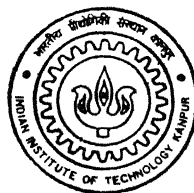This is to certify that the present work entitled "Mechanical Testing of Weld Simulated HSLA Steels" by Manjul Sarma has been carried out under our supervision and it has not been submitted else where for a degree

Dr N K Batra
Professor
Deptt of Materials & Met Engg
Indian Institute of Technology
KANPUR

Dr R Tandon
Assistant Professor
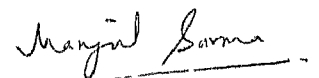Deptt of Materials & Met Engg
Indian Institute of Technology
KANPUR
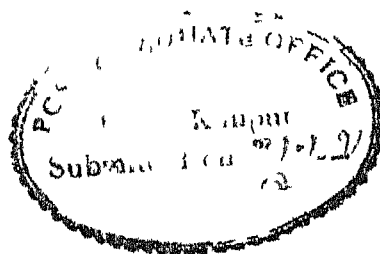
ACKNOWLEDGEMENTS

It gives me a great pleasure to express my deep sense of gratitude and indebtedness to my thesis supervisors Dr N K Batra and Dr R Tandon for their expert guidance and constant encouragement provided throughout the course of my work

I greatfully acknowledge Mr K S Tripathi, Mr K P Mukherjee, Mr B K Jain, Mr J L Kuril and Mr K K Malhotra for extending their kind cooperation at various stages of my experimental works

I am very much thankful to all of my friends who helped me during my works and made staying at IIT Campus enjoyable

Finally, I would like to express my appreciation to my exuberant wife Anita, without her constant encouragement and support the M Tech program would never has been completed

- MANJUL SARMA

ABSTRACT

Heat affected zone (HAZ) plays an important role in determining the properties of a weldment and hence the weldability of a metal Microstructural changes occur in the heat affected zone due to the thermal cycles experienced by a weldment In order to study the correlation between the cooling rate and mechanical properties of a material a weld simulation study was made in the laboratory for three different high strength low alloy (HSLA) steels The different test samples were simulated by keeping these rapidly into a furnace and then quenched in different cooling media The heating and cooling was done by a predetermined manner, so that it represents an actual weld thermal cycle Weld thermal cycle may be characterized by a peak temperature as well as cooling time from $800^{O}C$ to $500^{O}C$ in the heat affected zone Tensile strength, hardness and toughness properties were measured for simulated samples Scanning electron microscopy was used to study the fractography of the tensile test samples

Optical microscopy results show that steel samples when heated rapidly to $1100 - 1250^{O}C$ and water quenched within one second to cool from 800 to $500^{O}C$ show presence of martensite and bainite phases These samples showed elongation of about 7 pct and yield strength of 839 MPa Other simulated samples (forced air and air cooled) showed higher elongation but comparatively low yield strength This changes of mechanical properties is well

understood by its microstructural study Mixed structure of martensite, bainite, widmanstatten ferrite, acicular ferrite are formed at intermediate rate of cooling using forced air i e , 30 to 45 sec to cool from 800 to $500^{O}C$ Charpy impact testing of forced air cooled steel samples (time taken from 800 - $500^{O}C$ is 65 sec) give best results for toughness as compared to water quenched or annealed

CONTENTS

LIST OF FIGURES

LIST OF TABLES

NOMENCLATURE

C_{eq}	Carbon equivalent
C_p	Specific heat (J/kg-k)
H_f	Heat of fusion (J/kg)
k	Thermal conductivity (J/m-s-k)
k_s	Conductivity of solid material (J/m-s-k)
P_{cm}	Weld crack chemical composition index
Q	Strength of the heat source (J/s)
Q_g	Rate of heat generation per unit volume
T	Temperature (^{O}C)
t	time (s)
T_l	Liquidus temperature (^{O}C)
T_s	Solidus temperature (^{O}C)
T_{8-5}	Time taken to cool the material from 800°C to 500°C
$t_{>800}$	Time for which the material remains above 800°C
v	Velocity of the heat source (m/s)
w	Distance from the heat source
α	Thermal diffusivity (m^2/s)
ρ	Density (kg/m^3)

CHAPTER ONE

1   INTRODUCTION

Welding is an operation in which two or more parts are united by means of heat or pressure or both in such a way that there is continuity in the nature of the material (metal) between these parts A filler metal, whose melting temperature is of the same order as that of the parent material, may or may not be used [1] This secondary method of fabrication has been extensively used for assembling various structures such as bridges, high-rise building, storage tanks pressure vessels, ships, pipe lines etc Welding offers many advantages over riveting, in that air and water tightness, good joining effeciency, economical and without any limit to thickness of the parts to be joined

However, sometimes welding may create some problems such as cracking and the crack may lead to reduction of strength in the weldment Extensive research is being conducted for improving welding procedures and to obtain better mechanical properties of the weldment

In this study, we have focused our attention to some mechanical properties of the weldment under severe working conditions Peculiar thermal cycles undergone by welds due to localized moving intense heat source applied during welding leads

to reduction of strength and decrease of mechanical properties in the weldment The thermal cycle also cause in complex phase transformations in and around the welded joint producing a wide range of microstructures having different properties The type of resulting microstructure depends on many factors such as weld design, plate thickness, base metal composition and welding parameters such as current, travelling velocity, pre-heat temperature etc

In steels, weldability is determined by the microstructural changes that occur in the heat affected zone (HAZ) The composition of the base metal in the HAZ remains unchanged, whereas the composition of the weld metal is influenced by the composition of the filler metal and the degree of dissolution attained It is not very practical to study the microstructural changes that occurs in weldments due to interplay of many operating variables mentioned before In actual welds, the microstrcture and properties vary considerably from one location to another within the fusion and heat affected zones, depending on thermal history experienced at each point

The volume of the material corresponding to any given thermal history is quite small Therefore it is difficult to establish a specific structure - property relationship in actual welds So, a convenient method for this is to heat treating of the steel sample similar to those experienced in actual weld thermal cycle known as weld simulation technique Simulation can be carried out for each zone of welds thereby resolving the effect of

many other parameters The simulation results combined with analytical techniques can give useful information to optimize the weld properties

High strength low alloy (HSLA) steels are now becoming important structural materials because of its high strength, toughness at low temperature and simulataneously maintaining good weldability Weldability is defined in terms of susceptibility to the various types of cracking during welding fabrication and toughness at heat-affected zone (HAZ) [4]

The present study is carried out to evaluate the heat affected zone (HAZ) microstructure and mechanical properties of HSLA steel This is done by subjecting steel samples to thermal cycles of varying severity Variety of standard tensile and charpy test samples were simulated by keeping these in a furnace and then quenching in different media such as water, forced air and still air The most severe thermal cycle used (water quenched) was to simulate the microstructure and mechanical properties very close to the weld-metal zone Cycles with decreasing severity (air cooled) were used to study the properties of base metal as one traverses laterally away from the weld zone It is a very convenient method to study the microstructures, grain sizes, particularly mechanical properties because simulation gives only one type of microstructure

CHAPTER TWO

2 LITERATURE REVIEW

2 1   STRUCTURAL MATERIALS   HSLA STEELS

2 1 1   INTRODUCTION

High strength low alloy steels are a group of steels intended for structural application These steels have specified minimum yield strength of about 275 MPa and sometimes as high as 1035 MPa These steels contain small amount of alloying elements to achieve high strength in the hot-rolled or heat treated conditions [2]

2 1 2   PROPERTIES REQUIRED FOR HIGH STRENGTH STEELS

High strength steel plate possesses three fundamental properties They are high strength, toughness at low temperature and simultaneously having good weldability Weldability is difined in terms of susceptibility to various types of cracking during welding fabrication and toughness at heat affected zone (HAZ) These three fundamental properties are discussed below in brief

2 1 2.a Yield Strength

It is the stress corresponding to which material shows plastic deformation It is related to the grain size, degree of strain hardening, distribution of carbide and nitride particles etc Mathematically it may be described as follows [3]

4

$$\sigma_y = \sigma_o + k_y d^{-1/2} + k_y' d_{SG}^{-n} + k_A f_A \qquad (1)$$

where, d grain size, d_{SG} subgrain size, f_A the volume fraction of the second phase and k_y', k_y constants σ_o can be expressed as [2],

$$\sigma_o = \sigma_{lf} + \Delta\sigma_{ss} + \Delta\sigma_{ppt} + \Delta\sigma_{disl} \qquad (2)$$

where, σ_{lf} lattice friction, $\Delta\sigma_{ss}$ solid solution hardening, $\Delta\sigma_{ppt}$ precipitation hardening component and $\Delta\sigma_{disl}$ dislocation hardening component

2 1 2 b Low Temperature Toughness.

Low temperature toughness is represented by ductile-to-brittle transition temperature T_{rs} [2]

$$T_{rs} = A' - B d^{-1/2} - B' d_{SG} + f(z) \qquad (3)$$

where, z is a variable representing volume fraction and morphology of the second phase, and B and B' are constants, A' is given by the following factors

$$A' = A + \Sigma a_1 X_1 + \alpha \Delta \sigma_{ppt} + \beta \Delta \sigma_{disl} \qquad (4)$$

where X_1 is content of alloying element, a_1, α and β are constants and A is a correction factor

An examination of equation (3) reveals as that T_{rs} is governed by the matrix factor, grain and sub grain size factor, and the factors representing the character of the second phase. It is to be emphasized that all the strength factors decrease

toughness, except grain refinement and Ni - addition

2 1 2 c Weldability

The term weldability describes two different properties One is low temperature weld cracking which occurs during welding fabrication This cracking occurs due to the combined effects of hydrogen occluded in the HAZ, strain constraint at weld joint and residual tensile stress However, since hydrogen plays a major role in causing low temperature cracking, the crack is very often called hydrogen cracking The weld - crack susceptibility is given by P_C [3], where

$$P_C = P_{cm} + t/600 + [H] \tag{5}$$

where, t is the plate thickness in mm representing the degree of strain constraint and [H] is diffusible hydrogen in weld metal of 100 g P_{cm} is called weld - crack chemical composition index [3], and is given by

$$P_{cm} = C + \frac{Si}{30} + \frac{Mn}{20} + \frac{Cu}{20} + \frac{Ni}{60} + \frac{Co}{20} + \frac{Mo}{15} + \frac{V}{15} \tag{6}$$

P_C represents weld susceptibility (for the low alloy steels) to weld cracking (cold)

Carbon equivalent (C_{eq}) is also often used to describe the susceptibility to weld cracking However, C_{eq} is more suitable to describe the maximum hardness at HAZ, and accordingly ductility rather than crack suceptibility C_{eq} is given by [3],

$$C_{eq} = C + \frac{Mn}{6} + \frac{Cr + Mo + V}{5} + \frac{Ni+Cu}{15} \quad \text{(in wt \%)} \tag{7}$$

6

The other property of weldability is the toughness in HAZ, which governs the performance of weld - joint and thereby welded strcture Toughness at HAZ is markedly deteriorated due to coarse grain structure and the formation of brittle, hard martensite In general, strengthening of base metal through the additions of alloying contents definitily decreases toughness

2 1 3 Production Process for HSLA Steels

In order to meet the fundamental properties of HSLA steels such as higher strength, improved toughness, ductility and formability, and increased weldability, the carbon content is kept low (0 03 - 0 15) pct , moreover one or more of the strong carbide forming elements which are stable at high temperature such as vanadium, titanium and niobium along with a group of solid solution strengthening elements such as manganese and silicon are added to steel [2]

In order to meet the contradictory requirements of these steels, desired strength is achieved through refinement of ferrite grain size, produced by the additions of microalloying elements and in combination with various forms of thermo mechanical processing This procedure has made it possible to improve the resistance of steels to hydrogen assisted cold cracking, stress corrosion cracking (SCC), and brittle fracture initiation in the weld heat affected zone without lowering the base metal strength, ductility or low temperature toughness [2]

The bulk of structural steels may be produced by one of the following routes [4]

1   Hot rolling, without subsequent heat treatment,

2   Controlled rolling, i e , rolled at a temperature in a narrow range so that a fine grain size is produced

3   Direct normalising of hot rolled product e g forced air cooling

4   Normalizing of hot rolled product after cooling to ambient temperature

5   Quenching and tempering

6   Control quenching, to produce a bainitic structure

The most important process is the control rolled process where a careful control of time - temperature - deformation sequence is carried out The main purpose of controlled rolling is to refine grain structure and thereby increase both the strengh and toughness of steel in the hot rolled condition to a level equivalent to, or better than those of highly alloyed and quenched and tempered steels [4]

The presence of microalloying elements in low carbon steel would produce an extremely fine dispersion of small and stable microalloy carbides, nitrides and/or carbonitride precipitates which effectively influence the grain coarsening and cause pinning of austenite boundaries during controlled rolling Such steels subsequently transforms into a fine grained ferrite structure The controlled rolling practice for steels of suitable composition is shown schematically in Fig 2 1 [5]
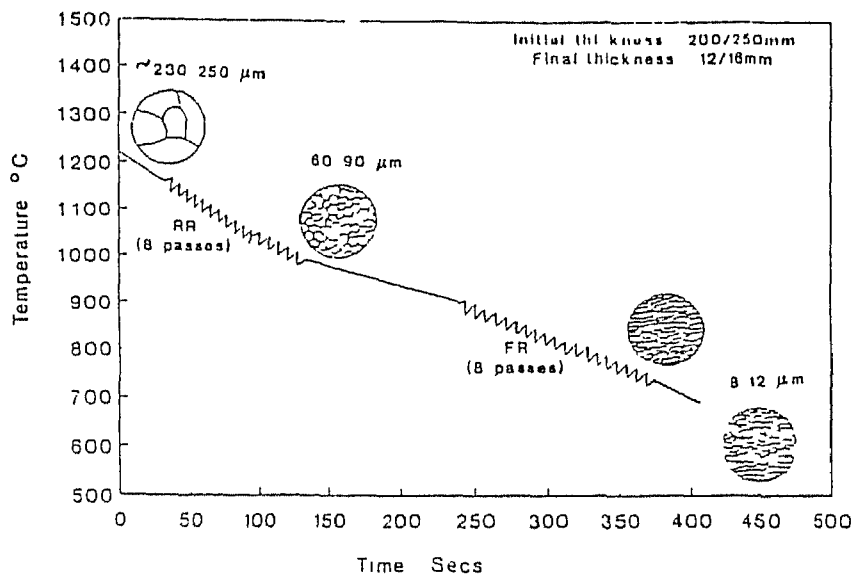
FIGURE 2 1   Typical presentation of TMPC schedule for controlled
             rolling of HSLA steels
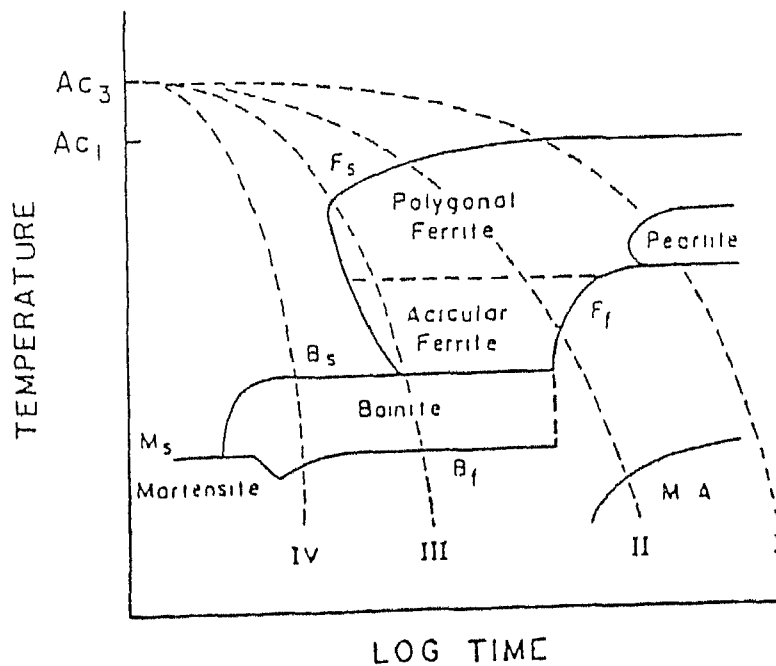
FIGURE   2 2   Schematic   CCT diagram for control   rolled   HSLA
          steels

Presence of manganese suppresses austenite to ferrite transformation temperature and retards the rate of transformation thereby leading to refinement of the ferrite grain size [5] Addition of (1 5 - 2 0) percent of manganese may produce acicular or bainitic structures In case of Niobium and Vanadium, carbonitrides of these elements may precipitate in austenite during transformation, or in the ferrite after transformation is complete [4]

The transformation behaviour of a control rolled microalloy steel may be represented by critical cooling transformation (CCT) diagram as shown in Fig 2 2 The transformed microstructure may include pearlite, polygoral ferrite, acicular ferrite, bainite and martensite depending on the processing route and steel chemistry

The major strengthening mechanism in control rolled HSLA steels includes the following [4]

1   Grain refinement
2   Precipitate hardening by strain enhanced precipitation of microalloy carbonitrides in ferrite
3   Solid solution strengthening from Mn, Si and uncombined nitrogen
4   Dislocation substructure strengthening

For example the contribution to strength suggested for a Nb microalloyed control rolled is given in equation (8)

$$\sigma_y(550 \text{ MPa}) = \sigma_1(6\%) + \sigma_{\text{solid soln}}(25\%) + \sigma_{\text{ppt hard}}(6\%)$$

$$+ \sigma_{\text{text}}(8\%) + \sigma_{\text{disl}}(8\%) + kd^{-1/2}(47\%) \qquad (8)$$

The grain size achieved through control rolled process is around 5 - 9 μm [5]

2 2 The Weld-Thermal Cycle

Arc welding is a process in which a very intense moving heat source is applied to the work piece By studying heat flow during welding, useful results can be obtained Many investigators have made detailed study of heat flow in welding The solutions obtained are useful in predicting thermal cycles and base metal and hence in predicting microstructure of heat affected base material and other related problems associated with welding

The basic equation to describe heat flow in a solid body i e Laplace equation is given as follows -

$$\frac{\delta T}{\delta t} = \frac{1}{\rho C_p} \left[\frac{\delta}{\delta x}\left(k\,\frac{\delta T}{\delta x}\right) + \frac{\delta}{\delta y}\left(k\,\frac{\delta T}{\delta y}\right) + \frac{\delta}{\delta z}\left(k\,\frac{\delta T}{\delta z}\right) \right] + Q_g \qquad (9)$$

where,

T = Temperature (k)

t = Time (S)

k = Thermal conductivity (W/m-k)

C_p = Specific heat (J/Kg-k)

ρ = Density (kg/m^3)

x,y,z = Coordinates in three perpendicular directions (m)

Q_g = Rate of heat generation per unit volume of the body

$(J/s-m^3)$

Rosenthal [6] was the first to report an analytical solution by making the following assumptions

1   The heat source moves with a constant speed along a line on the surface of a large body

2   Thermal properties of the material remain constant

3   No heat is lost by radiation and convection to surroundings

4   Quasi steady state is reached, i e , temperature distribution with reference to heat source does not change with time

Rosenthal modified the differential equation for a quasi stationary state w r t moving coordinates and obtained the following

$$- V \frac{\partial T}{\partial w} = \alpha \left[\frac{\partial^2 T}{\partial w^2} + \frac{\partial^2 T}{\partial y^2} + \frac{\partial^2 T}{\partial z^2} \right] \qquad (10)$$

where,

$w = x-vt$ (10 a)

$\alpha = [k/\rho C_p]$ (10 b)

$\quad =$ Thermal diffusivity of the solid (m^2/s)

$\rho =$ Density of solid (kg/m^3)

$w =$ Distance from heat source in x-direction (m)

$v =$ Velocity of heat source

$t =$ Time (S)

Rosenthal solved equation (10) under a few simple cases, and these are tabulated below -

Table 2 1 Expression for analytical solution of heat flow

Plate Thickness	Type of heat flow	Expression for analytical solution of heat flow
Thick	3-dimensional	$T - T_o = \dfrac{Q}{2\pi k}\, e^{-(v/2\alpha)w}\, \dfrac{e^{-(v/2\alpha)R}}{R}$ *
Finite thickness	2 5 dimensional	$T - T_o = \dfrac{Q}{2\pi k}\, e^{-(\frac{V}{2\alpha})w}\left[\dfrac{e^{-(\frac{V}{2\alpha})R}}{R} + \sum\limits_{n=1}^{\infty} \dfrac{e^{-(\frac{V}{2\alpha})R_n}}{R_n}\right.$ $\left. + \dfrac{e^{-(\frac{V}{2\alpha})R_n'}}{Rn'}\right]$ **
Thin	2-dimensional	$T - T_o = \dfrac{Q/s}{2\pi k}\, e^{-(\frac{V}{2\alpha})w}\, k_o\left(\dfrac{V}{2\alpha}\, r\right)$ ***

*

$$R = \sqrt{w^2 + y^2 + z^2}$$

Q = Strength of the heat source (J/s)

**

$$R_n = \sqrt{[\,w^2 + y^2 + (2nt - z^2)\,]}$$

$$R_{n'} = \sqrt{[w^2 + y^2 + (2nt + z)^2]}$$

t - plate thickness

***

$$r = \sqrt{w^2 + y^2}$$

K_o = is modified Bessel function of the second kind and zero order

S = plate thickness

2 3 NUMERICAL MODELING OF HEAT FLOW IN WELDS

With the development of numerical techniques and availability of low cost powerful computational devices, it was no longer necessary to make idealized assumption that were required in determining the analytical solution Thermal properties of the materials to depend on temperature Further it sounds impractical to ignore the phase change effect and heat lossess from the surfaces

Pavelic and Tarbakuchi [7] solved the basic equation using a finite difference technique assuming linear terms to be dominant The result obtained by numerical method was compared with that measured experimentally The temperature distribution in the weldment predicted by this technique was much more accurate than those predicted by other numerical techniques Pavelic and Tarbakuchi assumed the distribution around the heat source was

$$q(r) = q(o) e^{-C_c r^2} \qquad (11)$$

Where,

$q(r)$ = Surface flux at radius $r (w/m^2)$

$q(o)$ = Maximum flux at the centre of the heat source (w/m^2)

C_c = Concentration coefficient

r = Radial distance from the centre of the heat source

Papazoglou and Masubushi [8] developed a model using finite element method for analyzing temperature distribution Further they extended the model to study the thermal stress

distribution and residual stresses In this solution they considered convective and radiative heat loss from the boundary They considered a nonuniform mesh size and placed finer mesh size elements near the weld centre because of the large thermal gradient there They also took into account the temperature dependance of the thermal properties

Goldak, Bibby and Moore [9] developed a finite element formulation for trancient heat flow problem This finite element method is based upon a piece wise polynominals approximation for the temperature field within each element which are to written as follows

$$T (x, y, z, t) = \sum_{i=1}^{nodes} N_i (x, y, z) T_i(t) \qquad (12)$$

Where,

N_i are basic functions dependent only on the type of element and its size and shape

$T_i(t)$ are the nodel values of the temperature at time t, which can be evaluated by using Galerkin's FEM

The results obtained from the above heat flow models using numerical techniques were found to closely approximate the experimental results

Patro [10] solved the differential heat flow equation numerically to determine the temperature profile as a function of position and time in the weldment For this purpose the partial

15

differential equation is converted into a set of discretized equations by using the explicit finite difference technique, which was used to study the effect of various operating parameters on the thermal profile experienced by the base plate

The parameters that had been used for computer simulation study are -

1   Preheat temperature, T_{ph}
2   Strength of the heat source, Q
3   Speed of the source, V

Thermal data used in model are shown in Table 2 2 a and details of the different run conditions are mentioned in Table 2 2 b

Table 2 2 a   Thermal data used in the model

Variable	Value
k_s	49 6 J/m sk
ρ	7850 kg/m^3
c	529 J/kg k
H_f	275000 J/kg
T_1	1500°C
T_s	1400°C
k_1/k_s	4
Plate	150 x 60 x 20 mm^3

Table 2 2 b   Run conditions

Q (kw)	V (mm/s)	T_{ph} (°C)	t_{8-5} (s) z = 4 mm	$t_{>800}$ (s) z = 4 mm
4	2	25	5 8	7 90
4	6	25	2 12	1 43
4	12	25	0 70	0 30
2	2	25	3 48	3 00
8	2	25	19 01	16 22
4	2	200	5 80	7 90
4	2	300	5 67	7 96
4	2	25	13 30	10 60
4	2	25	48 60	12 90

From the data in tables a family of isotherms around the heat source in the tempeature range of 750 - 1500°C are shown in Fig 2 3 a and 2 3 b for different combinations of operating parameters

2 4   WELD SIMULATION TECHNIQUE

Weld simulator (commercially known as Gleeble simulator) have been developed to simulate the weld thermal cycle under laboratory condition in order to obtain information about microstructure and property changes in heat affected zone and, are usually done by registance heating and water cooling of samples Control of thermal cycle (which is based on Rosenthal's heat flow theory) is via a Pt/Pt-13% Rh thermocouple spot welded
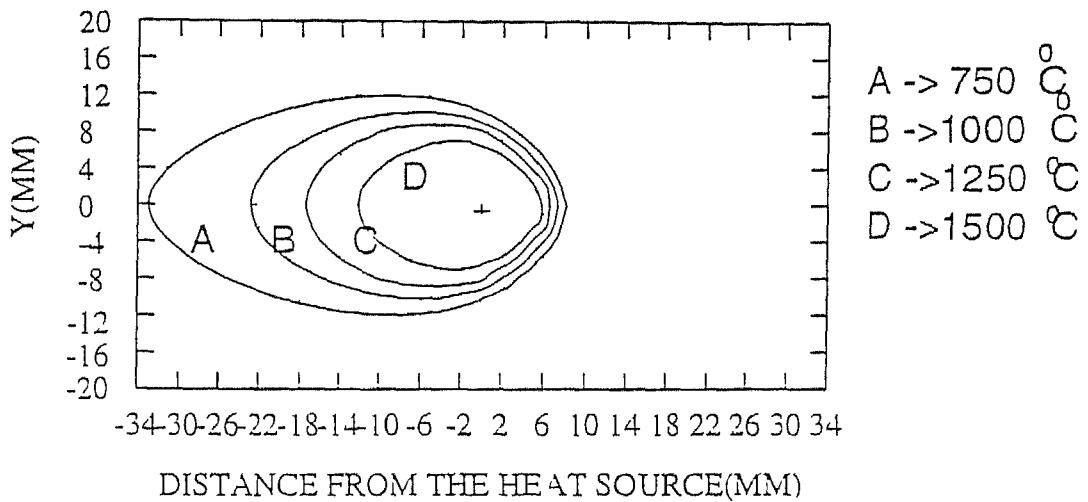
a) xy plane (Top surface)

$Q = 8KW$ $v = 2mm/S$ $T_{ph} = 25^0C$ $b = 6mm$

b) yz plane (Beneath the weld line)

Figure 2 3a Typical isotherms computed for certain welding condition

A -> 750 ^{o}C
B -> 1000 ^{o}C
C -> 1250 ^{o}C
D -> 1500 ^{o}C

a) xy plane   (Top surface)

A -> 750 ^{o}C
B ->1000 ^{o}C
C ->1250 ^{o}C
D ->1500 ^{o}C
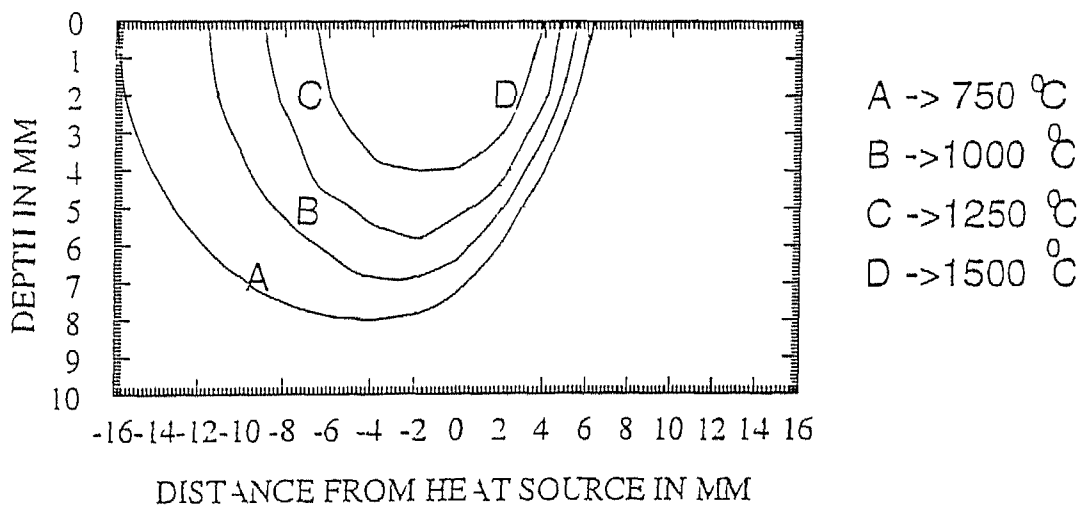
Q = 4KW v= 2mm/S T_{ph} = 25 ^{o}C b = 6mm

b) yz plane (Beneath the weldline)

Figure 2 3b Typical isotherms computed for cetain welding condition

19
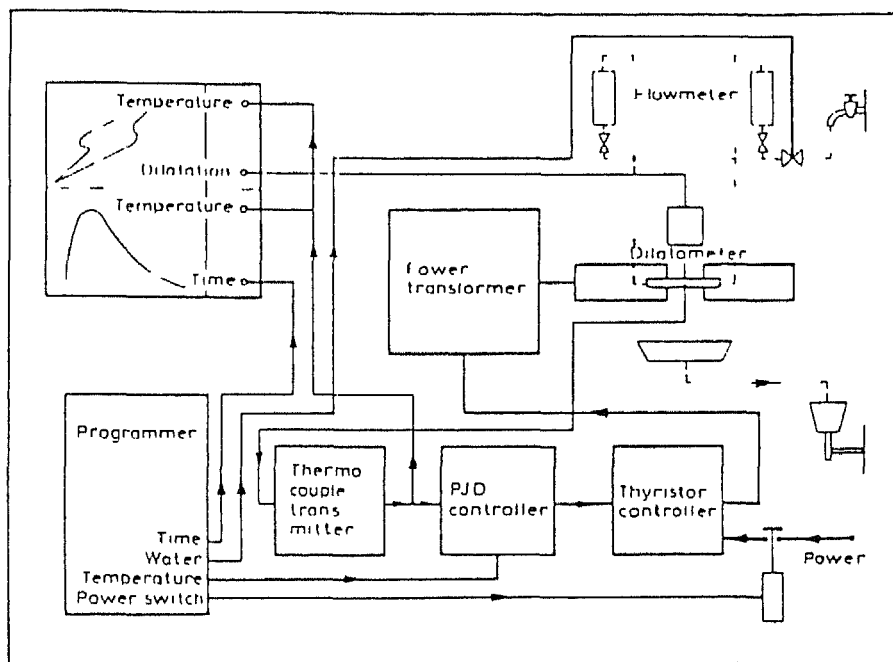
FIGURE 2 4 Schematic layout of weld thermal simulator equipment(3)

to the specimen's surface [4] It is possible to program the required thermal cycle to any required temperature-time profile, and to plot this thermal cycle and record phase transformations using a dilatometer [4] (Fig 2 4)

The simulation of weld heat affected zone microstructures by means of gleeble thermal/mechanical simulator [11] has become widely accepted throughout welding industry

Various researchers did simulations for different purposes, Kobayashi [12] in his work simulated HAZ structure in 16mm diameter and 55mm in length by heating the sample in a induction furnace upto 1350°C and held at that temperature for 5 sec and cooled to room temperature to achieve t_{8-5} of 90 sec He found that the specimen had the uniform temperature of 5mm in the centre and specimen were machined for charpy impact test

Bowker et al [12] had studied the effect of weld thermal cycle on behavior of Ti - Nb carbonitrides in HSLA steels A bead on plate weld technique was used to simulate the weld thermal cycle

Godden and McGrath [14] in their study compared the notch toughness of weld HAZ with Gleeble simulated HAZ They found a close agreement between the properties of two HAZ structures But they found that Gleeble simulation will be inadequate to measure noted toughness of low energy weld as the heat affected zone is very narrow

2 5 Structural changes due to weld thermal cycles

A weldment is composed of mainly three regions viz

1   Weld metal

2   Heat affected zone

3   Unaffected base metal

WELD METAL

The weld metal is that part of the weldment that has melted and resolidified during the welding operation The microstructure and properties of weld metal depends on complex interaction between several important variables such as the total alloy content, the concentration of different solute elements, prior austenite grain size and weld thermal cycle [9]

HEAT AFFECTED ZONE

The heat affected zone (HAZ) is that part of the base metal adjacent to the weld metal which has been heated during welding to a high temperature It has undergone significant and detectable structural change, but has generally not become molten The properties of the region are determined by the austenite grain size, matrix composition and cooling rate The precipitation will be effective in restricting grain growth unless it coarsen or dissolved into the matrix Depending on steel composition, Nb(CN) can restrict grain growth upto temperatures of $1200 - 1250^{O}C$ whereas V(CN) is effective only upto $900^{O}C$ [4]

The time span to cool from $800^{\circ}C$ to $500^{\circ}C$ in the weldment (t_{8-5}) has now been widely adopted in welding research [16] Most of the transformations in the plain carbon steels occur in the temperature interval of 800 - $500^{\circ}C$ and time of cooling in this temperature range is critical

Depending on the peak temperature that has reached, the heat affected zone can be divided into four distinct zones [15] These are

1   Coarse - Grained HAZ (CGHAZ), adjacent to the fusion line

2   Fine-Grained HAZ (FGHAZ), above Ac_3 and below grain coarsening temperature

3   Inter-critical HAZ (ICHAZ), between Ac_1 and Ac_3 temperature range

4   Sub-critical HAZ (SCHAZ), below Ac_1 temperature

Different sub-zones of HAZ are shown in Fig 2 5

COARSE-GRAINED HAZ

This zone experiences peak temperatures between $1100^{\circ}C$ and $1450^{\circ}C$ Temperature of this range produces a coarse grained austenite which because of low density of grain boundaries, tends to preclude extensive transformation to ferrite during cooling Further peak temperature of this order causes dissolution of all the precipitates thus increasing the hardenability of steel [15] Phases that are observed in this region include equiaxed or
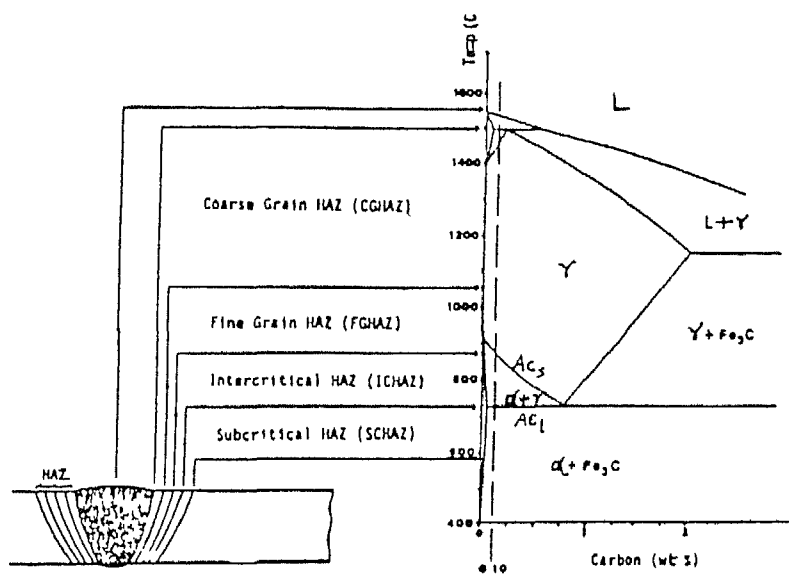
FIGURE 2 5 HAZ regions superimposed on the Iron-Carbon diagram

polygonal ferrite, widmanstatten ferrite, bainitic ferrite and lathe martensite In addition, the carbon enriched phases or minor phases associated with the above mentioned ferrites may transform to pearlite, degenerated pearlite, carbides or martensite - austenite (M - A) Fig 2 shows CCT diagram applicable to a CGHAZ region in a C-Mn-Si-Al-Nb steel [17] Brownrigg and Boelen [18] observed that at a cooling rate corresponding to shielded arc welding (SAW) at 3 5 kJ mm^{-1} on a plate of 50 mm thick, the microstructure is bainite

FINE-GRAINED HAZ

This zone corresponds to a peak temperature in the temperature range of 850 - 950°C At these temperatures Nb(CN) restricts the grain-growth of austenite The austenite grain size is small and equiaxed which leads to the formation of polygonal ferrite

INTER-CRITICAL HAZ

This zone corresponds to a peak temperature between Ac_1 and Ac_3 Only the carbon rich constituents form austenite

SUB-CRITICAL HAZ

This zone corresponds to a peak temperature below Ac_1 Growth of precipitate particles, dislocation annihilation and strain aging are the only processes that are effective in this temperature range

The heat treatment given to a metal during welding produce different metallurgical structures which influence the mechanical properties of the metal So it is extremely essential to study the mechanical behaviour of materials such as strength, ductility, toughness, hardness etc along with their microstructural study Many researchers have adopted different techniques to assess the different zones of weldment

Gianetto et al [19] made a detailed assessment of the influence of composition and energy input on the structure and properties of single-pass submerged arc bead-in-groove welds produced on HY80 and HSLA80 steels Dilution from the base plate produced a marked variation in weld metal composition between the HY80 and HSLA 80 series of welds, which resulted in major differences in microstructure and mechanical properties The low - temperature notched toughness was poor for both the 1 and 4 kJ/mm welds with an improvement observed at intermediate energy input The poor notch toughness at 1 kJ/mm was attributed to the formation of hard lath martensite with high yield strength Intermediate energy input welds consisted of fine bainite microstructure with lower yield strength, which provided improved notch toughness The HSLA80 welds showed a small decrease in yield strength with increasing energy input and superior notch toughness indepdendent of energy input This occured as a result of the transformation to a high proportion (80%) of acicular ferrite with limited continuous/discontinuous grain boundary ferrite All of their results are tabulated below -

Table 2 3 Chemical Compositions of High-strength Steels and
Welding Electrode

Material	C	Mn	Si	S	P	Ni	Cr	Mo	Cu	Nb
HY80	17	30	19	014	007	2 59	1 53	42	03	005
HSLA80	06	50	27	004	007	92	66	25	1 02	004
HY80 MIL-S-16216J	12-18	10-40	15-35	002-020	020	2 00-3 25	1 00-1 80	20-60	0 25	-
HSLA80 MIL-S-24645A	06	40-70	40	006	020	0 70-1 00	0 60-0 90	15-25	1 00-1 30	02-06

Table 2.4 Tensile Properties of Submerged Arc Bead-in-groove
Welds Deposited in HY-80 Steel

Weld No	Energy Input (kJ/mm)	Yield Strength (MPa)	Ultimate Strength (MPa)	Elongation (%)	Reduction in Area (%)
HY80-1	1	875	1124	18	54
HY80-2	2	745	930	24	57
HY80-3	3	680	858	25	64
HY80-4	4	666	867	25	63

Table 2 5   Tensile properties of submerged Arc Bead-in-groove
Weld Deposited in HSLA-80 Steel

Weld No	Energy input (kJ/mm)	Yield Strength (MPa)	Ultimate Strength (MPa)	Elongation (%)	Reduction in Aver (%)
HSLA80-1	1	640	806	25	64
HSLA80-2	2	618	756	28	66
HSLA80-3	3	607	720	27	65
HSLA80-4	4	595	710	28	65

Fairchild et al [15], had studied intercritical HAZ microstructure and toughness in HSLA steels Two microalloyed HSLA steels were welded by the submerged arc process and ICHAZ toughness was assessed by using the Charpy and crack tip opening displacement (CTOD) tests Optical, scanning electron microscopy (SEM), and transmission electron microscopy (TEM) were used to study base metal and ICHAZ microstructure

One of the steels suffered severe toughness degradation in the ICHAZ as measured by the CTOD test It was determined by TEM that the only significant low-toughness facture in the ICHAZ was due to the presence of Martensite - Austenite (M-A) islands The formation of M-A was believed to be caused by a high amount of vanadium and silicon in solid solution, which increased

hardenability

The Charpy data showed the difference between the ICHAZ toughness of the steels, whereas, the CTOD results showed a distinct difference Charpy Testing may be insensitive when the microstructure varies over small distances, as is the case for weld HAZs

CHAPTER THREE

3 PLAN OF WORK

The primary objective of this study was to simulate weld heat affected zones in HSLA steels having two different compositions and to characterize their microstructure and mechanical properties

3 1 SIMULATION

Weld thermal cycles are characterized by peak temperature as well as cooling time The coarse-grained HAZ are the most dangerous part of the weldment Hence peak temperatures of $1250^{O}C$, $1200^{O}C$ and $1100^{O}C$ were selected for simulation studies The standard tensile-test samples and charpy test samples were simulated by keeping these samples in a furnace to the required temperatures and then quenching in different media such as ice water, water at room temperature, forced air and still air

3 2 CHARACTERIZATION

Tensile and impact tests were performed for evaluating the mechanical properties The broken pieces were subjected to fractographic study using the scanning electron microscope Weld simulated samples were subjected to hardness measurements as well as optical microscopy studies

3 3 ANALYSIS OF RESULTS

Results of simulation and mechanical testing were analysed to interpret their microstructural features and mechanical properties The practical utility of these results were enumerated Conclusions and suggestions for future work are given at the end

CHAPTER FOUR

4   EXPERIMENTAL PROCEDURES

Details of experiments designed to simulate heat affected zone and to carry out welding of HSLA steels are presented in this chapter This includes microstructural characterization and mechanical testing

4 1   MATERIALS

The compositions of HSLA steels used in the study are shown in Table 4 1 These steels were obtained from Bhilai Steel Plant and TISCO, Jamshedpur The steels from Bhilai Steel Plant are commercially termed as SAIL-MA steels and processed through LD-CONCAST-CONTROLLED ROLLED with accelerated cooling route

4 2   EQUIPMENT

The following equipments were used in the experimental work

Annealing Furnace

The 'OKAY' molybdenum disilicide resistor heated electric furnace with maximum working temperature of 1700° and with 15x15x30 cm working space was used for annealing of steel samples The accuracy of temperature controller is $\pm 5^{O}C$

Simulation Furnace·

Simulation work was carried out using a vertical tube silicon carbide resistance furnace The schematic diagram of the furnace is shown in Fig 4 1 The maximum working temperature of the furnace is 1400°C

Table 4 1 Composition of HSLA Steels (wt.%)

Steel	Source	Plate Thickness (mm)	C	Mn	Si	P	S	Al	Nb	N$_2$ (ppm
A	SAIL,(SAILMA) Bhilai	10	0 10	1 20	0 25	0 03	0 025	0 04	0 043	-
B	TISCO,(E-34) Jamshedpur	4	0 06/ 0 08	0 08/ 0 60	0 08 max	0 025 max	0 025 max	0 025/ 0 06	0 01/ 0 02	90 max
C	-do- (TISTEN-55)	10	0 12/ 0 16	1 2/ 1 4	0 10 max	0 030 max	0 025 max	0 02/ 0 07	0 02/ 0 03	100 max

Cutting Wheel All cutting operations were done by a Buchler silicon carbide wheel cutter

Universal Testing Machine Screw-driven Instron-1195 floor model was used to perform all tensile tests of the simulated sample

Leitz Metallux 3 Optical microscope was used for optical microscopy

JOEL JSM 840A Scanning Electron Microscope was used for fractography

Rockwell Hardness Testing Machine Rockwell hardness testing

machine was used to measure the hardness of the simulated test samples

Pt-Pt 10% Rh Thermocouples Connected to digital multivoltmeters were used to measure the temperature of the furnace

Chromel-Allumel Thermocouples Connected to Blue-Bell temperature indicator were used to measure temperature of the samples

Spot Welding MEW spot welding machine was used for spot welding the thermocouple to the samples

Grinding Wheel 'Wolf'- make abrasive grinding wheel was used for all grinding operations

Digital Millivoltmeters

Air-compressor and blower to generate forced air

4.3 PROCEDURES

4 3 1 SAMPLE PREPARATION

(1) About 24 standard tensile test samples were cut from the plate A and B received from SAIL, Bhilai and TISCO, Jamshedpur Dimensions of standard tension test specimens are shown in Fig 4 3

(2) About 13 charpy-test samples were made from plate A and C Dimensions of standard charpy test samples are shown in Fig 4 4
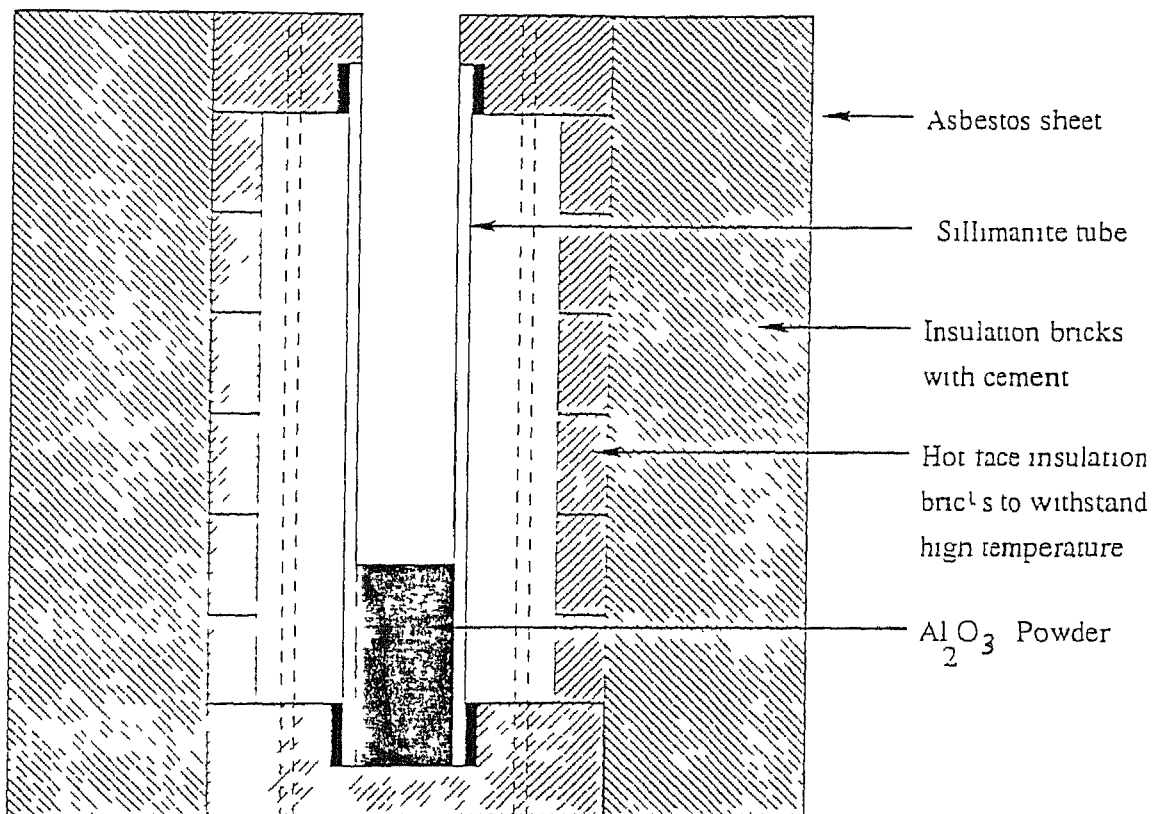
Figure 4 1 Schematic of the simulation furnace used

Figure 4 2 Chromel-allumel thermocouples spot welded to the steel sample

G - Gauge Length   25 0 $\pm$ 0 08 mm

W - Width   6 25 $\pm$ 0 05 mm

T - Thickness   plate thickness(6mm & 4mm)

R - Radius of fillet   6 (min) mm

L - overall length   100 mm

A - length of reduced section   32 mm

B - length of grip section   32 mm

C - width of grip section   10 (approx) mm

Fig 4 3   Rectangular tension-test specimens[from ANSI/ASTM Standard A 370-77]

Fig 4 4   Types of specimens for Charpy (simple beam) impact tests (Based on information in ASTM specification E 23)

4 3 2   HEAT TREATMENT

The following annealing cycles was given to the both tensile and charpy test samples

The samples were annealed at $1000^{O}C$ for approximately one hour under free flowing argon   Samples were cooled in the furnace under argon atmosphere upto $500^{O}C$ and thereafter they were withdrawn and allowed to cool in air
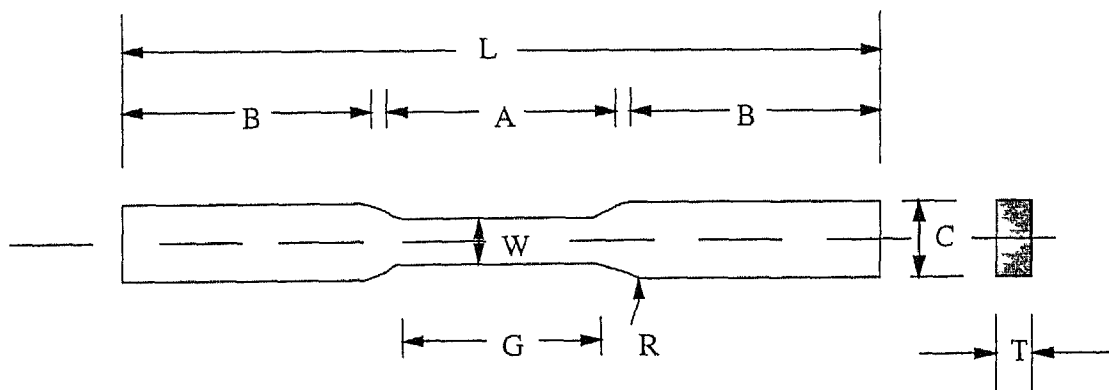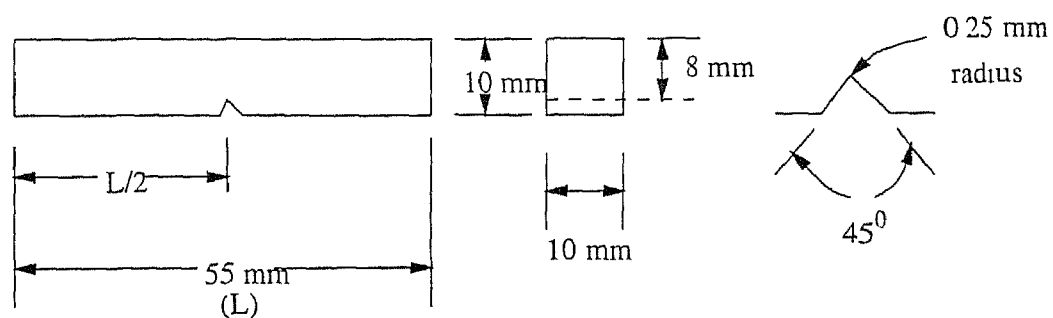
4 3 3   SIMULATION OF WELD THERMAL CYCLES

A chrommel-alumel thermcouple was attached to the sample by spot welding to record temperatures (Fig 4 2)   It was connected to a temperature indicator to monitor the heating and cooling rates of the specimen

The following procedures was used for simulation

1   Each sample was rapidly introduced into a high temperature furnace maintained at approximately $50^{O}C$ above the temperature desired in the specimen

2   The sample was kept in the furnace till the required peak temperature ($1100^{O}C$ or $1200^{O}C$) was reached

3   The sample was rapidly removed from the furnace and allowed to cool in a suitable medium to achieve the desired cooling rate

4 3 4   TENSILE TEST

The steel samples after the above treatment were ground to remove about 1 mm of the surface layer using an abrasive wheel This was done to ensure that there is no surface effect on microstructure and hardness of the sample Then the samples were tested in floor-mounted INSTRON-1195 universal testing machine at a cross head speed of 0 5 mm/min The gauge length and elongation measurements were made by making punch marks on samples

4 3 5   FRACTOGRAPHY

The tensile test samples which were fractured were cut to a length of 10 mm (along length) to study the fractured section in the scanning electron microscope (SEM) Fractography was carried out using SEM with attached camera

4 3 6   OPTICAL MICROSCOPY

Samples after tensile tests were mounted using a thermo setting compound for metallographic examination The surface of sample was grounded, polished and then etched with 5% nital solution Optical microscopy was carried out using Leitz Metallux-3 microscope with attached camera

4 3 7   TOUGHNESS TEST

The simulated standard notched specimens were tested by giving a simple blow by a pendulum swinging from a certain height The energy absorbed by various samples were noted

4 3 8   HARDNESS MEASUREMENTS

The hardness measurements of the simulated test samples were taken by Rockwell Test Machine Both Rockwell B and C scales were used for measurements In Rockwell B scale a 1/16 inch (1 6 mm) diameter steel ball with a 100-Kg major load and a 10-kg minor load was used whereas in Rockwell-C scale a diamond-point indentor with a 120° angle at the point, and 150 kg major load and a 10-kg minor load were used A total of 6 to 8 hardness measurements were taken on each simulated sample and the data averaged

CHAPTER FIVE

5 RESULTS

In this chapter the results of thermal cycle simulation, tensile testing of the simulated samples and charpy-notch test are presented

5 1 THERMAL CYCLES

The prepared samples from the plate were annealed by keeping the samples in the furnace at around $1000^{\circ}C$ for one hour in an inert gas atmosphere of argon and thereafter samples were allowed to cool slowly in furnace Thermal cycles for weld simulation experiments were designed for peak temperature of $1100^{\circ}C$, $1200^{\circ}C$ and $1250^{\circ}C$ corresponding to the coarse grained heat affected zone of the weldment The heating time, and time to cool from 800 to $500^{\circ}C$ i e t_{8-5} obtained by different cooling medium for each peak temperature are summarised in Table 5 1 for tensile testing and Table 5 2 for impact testing The difference in cooling times between the two test samples is due to the difference in their surface area

41

Table 5 1 Thermal cycles simulated for tensile testing

Sample No	Peak Temp T_p ($^{\circ}$C)	Time to reach T_{peak} (s)	Quenching Medium	Cooling time $t_{800-500^{\circ}C}$ (s)
(for SAILMA Steel)				
TA_{00}*	-	-	-	-
TA_{11}	1250	168 7	water	1
TA_{12}	1250	169 0	forced air	41 5
TA_{13}	1250	167 7	air	87 3
TA_{21}	1200	81 8	water	<1
TA_{22}	1200	81 0	forced air	38 5
TA_{23}	1200	82 0	air	84 6
TA_{31}	1100	58 0	water	1
TA_{32}	1100	57 8	forced air	35 5
TA_{33}	1100	56 5	air	76
(for E-34 Steel)				
TB_{00}*	-	-	-	
TB_{21}	1200	75 0	water	<1
TB_{22}	1200	73 0	forced air	41
TB_{23}	1200	72 0	air	83
TB_{31}	1100	48 0	water	<1
TB_{32}	1100	45 0	forced air	38
TB_{33}	1100	54 0	air	81

*As received condition

Table 5 2   Thermal cycle simulated for charpy impact testing

Sample No	Peak Temp (^{O}C)	Time to reach T_{peak} (s)	Quenching Medium	Cooling time 800-500°C(s)
(for SAILMA steel)				
CA_{01}**	-	-	-	-
CA_{31}	1100	69 8	water	1
CA_{33}	1100	68 0	air	124
(for TISTEN-55 steel)				
CB_{00}*	-	-	-	-
CB_{01}**	-	-	-	-
CB_{31}	1100	74 0	water	1
CB_{32}	1100	72 0	forced air	70
CB_{33}	1100	71 5	air	125
CB_{41}	1000	62 0	water	1
CB_{42}	1000	65 5	forced air	65
CB_{43}	1000	64 0	air	100

*   As received condition

** Annealed

5 2 MECHANICAL TEST RESULTS

The results of tensile and hardness testing on simulated samples of steel-A and steel-B are presented in Table 5 3 Ultimate tensile strength (UTS) is corresponding to the maximum load while yield stress refers to stress value for 0 2% offset Typical load deformation curves are shown in Fig 5 1

Table 5 3 Mechanical properties of weld simulated steel samples

| Samples	UTS (MPa)	YS (MPa)	Elongation (%)	Rockwell Hardness No (B and C scale)
TA_{00}	501 36	351 195	38 68	10 33Rc
TA_{11}	1092 57	973 85	09 646	40 77Rc
TA_{12}	552 14	437 05	22 185	20 10Rc
TA_{13}	529 531	395 28	26 076	13 5Rc
TA_{21}	970 37	838 98	07 00	36 35Rc
TA_{22}	518 24	396 38	25 69	16 00Rc
TA_{23}	520 70	370 80	27 55	09 55Rc
TA_{31}	1112 05	1044 35	10 569	30 31Rc
TA_{32}	566 15	421 54	24 00	09 90Rc
TA_{33}	567 82	416 40	24 09	06 90Rc
TB_{00}	423 61	361 81	34 10	77 93Rb
TB_{21}	710 00	618 39	12 64	24 00Rc
TB_{22}	440 13	332 96	21 13	76 58Rb
TB_{23}	455 98	333 74	26 45	75 33Rb
TB_{31}	651 09	532 36	18 00	20 59Rc
TB_{32}	430 93	327 51	20 82	76 22Rb
TB_{33}	424 07	307 02	22 79	72 42Rb
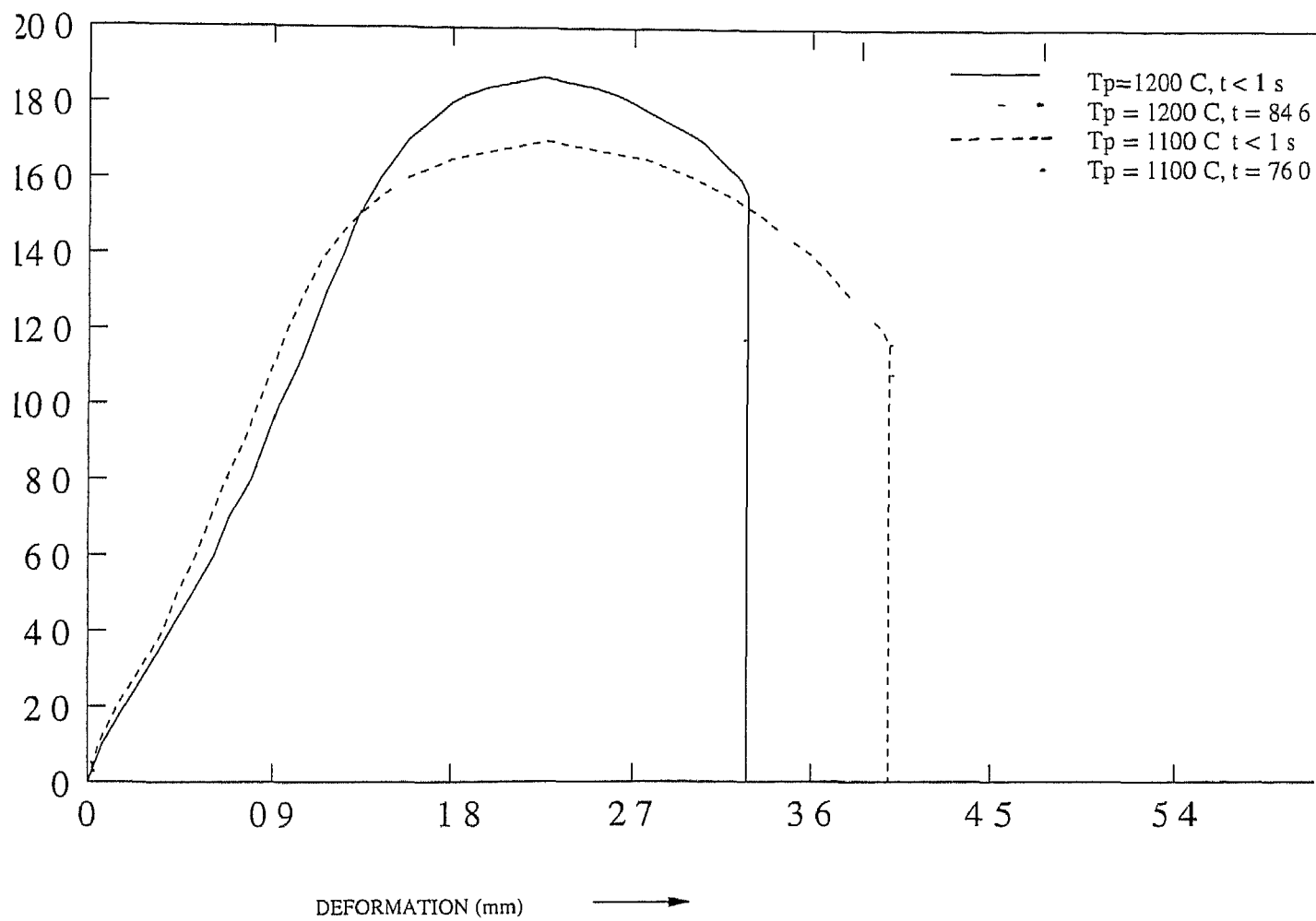
Fig 5 1 Typical load deformation curves obtained during Tensile Testing of 'Steel-B'

The result of weld simulated steel sample for charpy impact testing are summarized in Table 5 4

Table 5 4 Summary of hardness and Charpy test results of simulated steel samples

Sample No	Hardness		Charpy Test	
	Rockwell B	Rockwell C	Temperature $^\circ$C	Toughness(joule)
CA_{01}	68		25	212
CA_{31}	105	28	25	59
CA_{33}	80		25	304
CB_{00}	92		0	24
CB_{01}	82		0	41
CB_{31}	105	29	0	19
CB_{32}	80		0	43
CB_{33}	83		0	32
CB_{41}	97	20	0	22
CB_{42}	73		0	47
CB_{43}	83		0	39

Microstructures obtained in weld simulated test samples are shown in Fig 5 2 to 5 16 Observation made during microscopic examination of the simulated steel samples using optical microscope are given in Table 5 5

Table 5 5   Microstructures for simulated steel samples

Figure	Sample No	Microstructural observation	Micrograph No in Reference
5 2	TA_{00}	Banded structure due to rolling, Ferrite and pearlite	15 20 [21]
5 3	TA_{11}	Parallel fibres of massive martensite	320 [22]
5 4	TA_{13}	Pearlite in ferrite matrix, bainite is also seen	283 [22]
5 5	TA_{21}	Martensite, bainite and Widamanstatten ferrite	271 [22]
5 6	TA_{22}	Bainite in ferrite matrix small amount of pearlite is also seen	300 [22]
5 7	TA_{23}	Microstructure is similar to TA_{22} but the grain size is higher	134 [22]

5 8	TA_{31}	Fibres of massive martensitic structure	324	[22]

5 9 and 5 10	TA_{32} and TA_{33}	Pearlite and ferrite	136	[22]

5 11	TB_{00}	Ferrite and pearlite	167	[22]

5 12	TB_{22}	Bainite in Ferrite matrix	165	[22]

5 13	TB_{23}	Similar to TB_{22} but the grain size is larger	164	[22]

5 14	TB_{31}	Temper martensite, Parallel fibres of martensitic structure	323	[22]

5 15 and 5 16	TB_{32} and TB_{33}	Ferrite and pearlite	64	[22]

5 5 FRACTOGRAPHY

Microscopic examination of the fractured surface of the simulated steel tensile test samples using scanning electron microscope (SEM) are presented here

Fig 5 17 shows fractograph for the simulated E-34 steel during its tensile testing, corresponding to $T_{peak}=1200^{O}C$ and $t_{8-5} = 1$ s The scanning electron micrograph shows ductile fractured surface The dimpled structure indicates that plastic deformation takes place before fracture

Fig 5 18 shows fractograph for the simulated tensile test sample ($T_{peak}= 1100^{O}C$, $t_{8-5}= 81$ s) It also shows ductile - fracture surface The dimples are deeper than those seen in Fig 5 17 It is observed that number of dimples per unit area is more when t_{8-5} is low i e , for fast cooling rate Fig 5 19 shows how the grains are elongated near the fractured section compared to the grains which are away from the fractured section
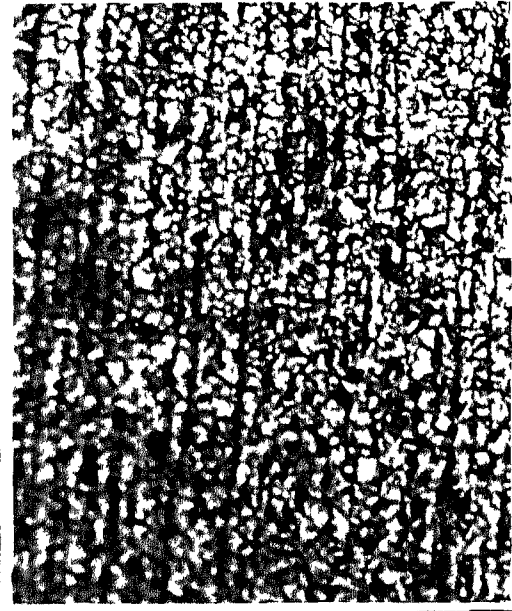
Fig 5 2   Optical micrograph of steel A
          as received condition, X200

Fig 5 3   Optical micrograph of simulate steel A
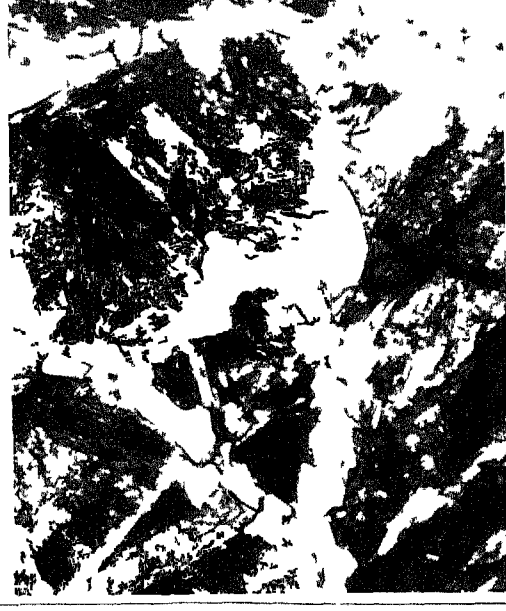   sample T_p = 1250°C, t_{8-5} < 1 s, X500

Fig 5 4   Optical micrograph of simulated steel A
          sample T_p = 1250°C, t_{8-5} = 87 3 s, X500

Fig 5 5   Optical micrograph of simulated steel
          sample T_p = 1200°C, t_{8-5} = 1 s, X500

Fig 5 6   Optical micrograph of simulated steel A
sample T_p = 1200°C, t_{8-5} = 38 5 s, X200

Fig 5 7   Optical micrograph of simulated steel
sample T_p = 1200°C, t_{8-5} = 84 6 s, X2C

Fig 5 8   Optical micrograph of simulated steel A
sample T_p = 1100°C, t_{8-5} < 1 s, X200

EINT -L LI R4U
II i KANPUR

 v₀ A .123160

Fig 5 9   Optical micrograph of simulated steel A
sample T_p = 1100°C, t_{8-5} = 35 5 s, X500

Fig 5 10 Optical micrograph of simulated steel A
sample T_p = 1100°C, t_{8-5} = 76 s, X500

Fig 5 11 Optical micrograph of steel B
as received condition

Fig 5 12 Optical micrograph of simulated steel B
T_p = 1200°C, t_{8-5} = 41 s, X200

Fig 5 13 Optical micrograph of simulated steel B
T_p = 1200°C, t_{8-5} = 83 s, X500

Fig 5 15 Optical micrograph of simulated steel B
$T_p = 1100^{\circ}C$, $t_{8-5} = 38$ s, X500

Fig 5 14 Optical micrograph of simulated steel B
$T_p = 1100^{\circ}C$, $t_{8-5} = 1$ s, X500
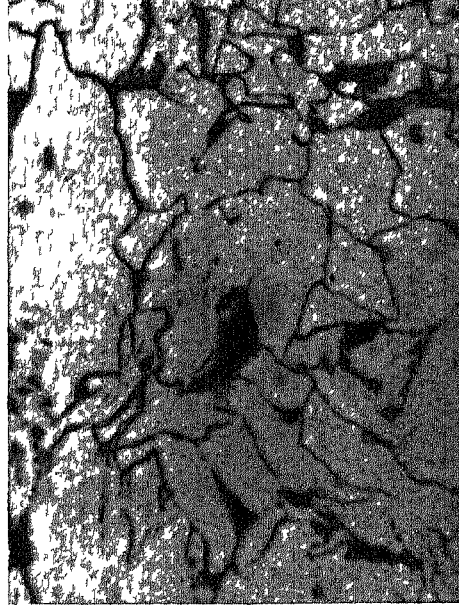

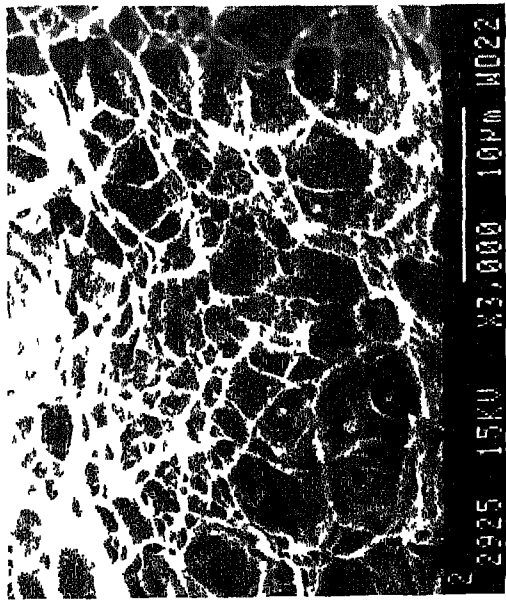Fig 5 16 Optical micrograph of simulated steel B
$T_p = 1100^{\circ}C$, $t_{8-5} = 81$ s, X500

Fig 5 18 Fractography for simulated steel B
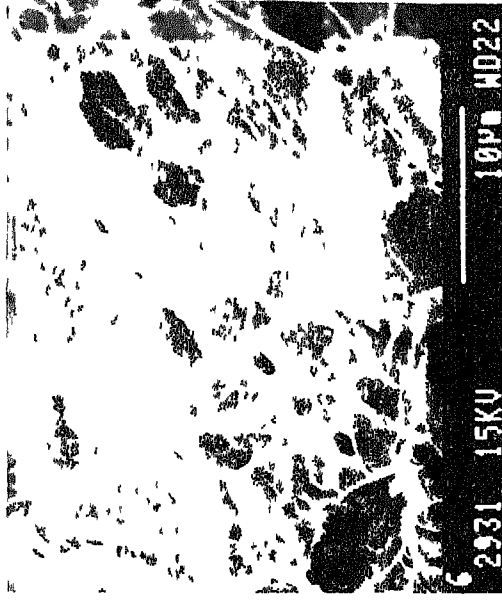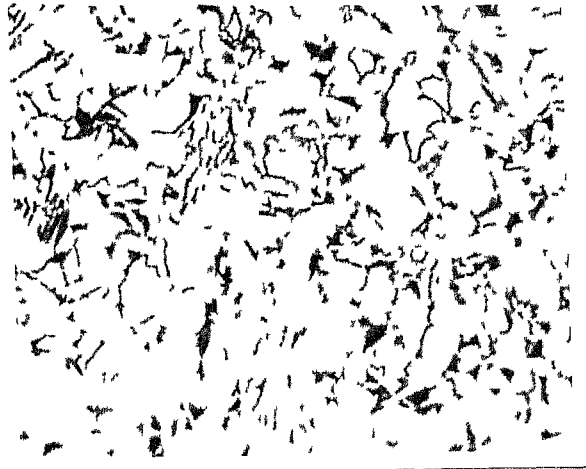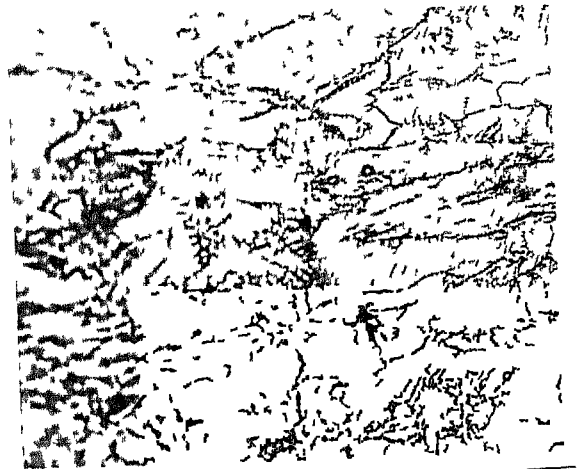$T_p = 1200^\circ C$, $t_{8-5} = 81$ s, X3000

Fig 5 17 Fractography for simulated steel B
$T_p = 1200^\circ C$, $t_{8-5} = 1$ s, X3000

(A)

(B)

(C)

Fig 5 19   Optical micrograph of simulated E-34 steel taken along
           the length of the tensile sample, micrograph (C) is
           nearest to the fractured section whereas is (A) is away

CHAPTER SIX

6 DISCUSSION

Routine mechanical testing of weld simulated samples shows that hardness value, tensile strength and yield strength all decrease and percentage elongation increases with the decrease in cooling rate Hardness, tensile strength, yield strength and percentage elongations data are plotted against cooing time $(t_{800-500^{\circ}C})$ in Fig 6 1 Only one set of data is plotted for clarity These results may be attributed to a greater extent of transformation of austenite to ferrite at lower cooling rate This in turn lowers the amount of martensite and bainite phases present in the steel Both martensite and bainite phases are well known to be hard and brittle, but bainite phase is more ductile than the martensite

Results of mechanical tests for water quenched samples, corresponding to t_{8-5} less than 1 sec shows that the hardness value increases with an increase in the peak temperature of weld simulated sample One set of data is plotted in Fig 6 2 One may expect that austenite grains are coarsened at a higher peak temperature It would take longer time for coarsened austenite to transform into ferrite when compared to fine grained austenitic phase obtained at lower peak temperature Also at a higher peak temperature, dissolution of carbides and nitrides of elements such as vanadium, titanium, niobium present in steel, is favoured
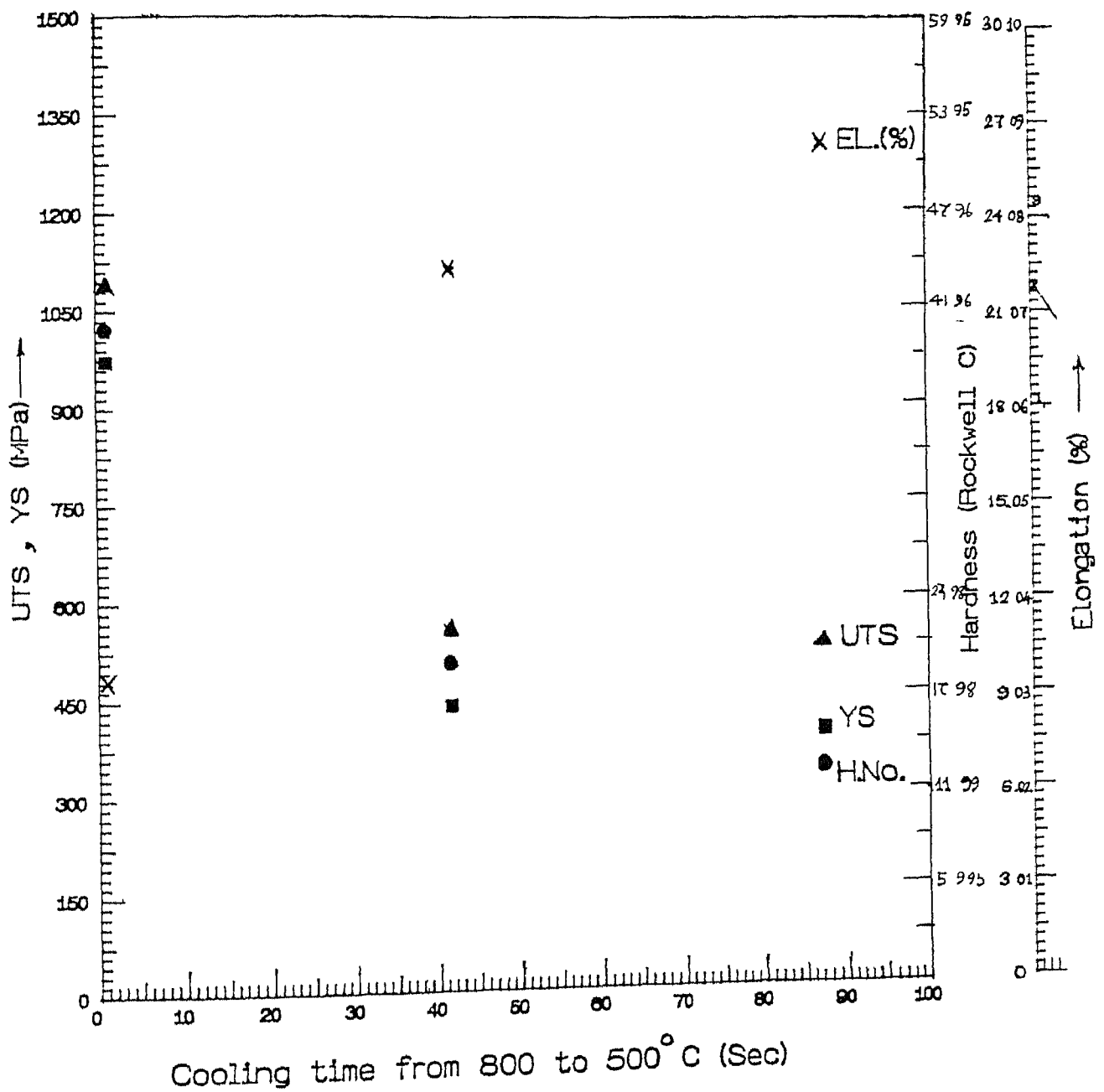
Fig 6 1   (UTS, YS, pct elongation, hardness) vs (t_{8-5}) for simulated steel A, T_p = 1250°C
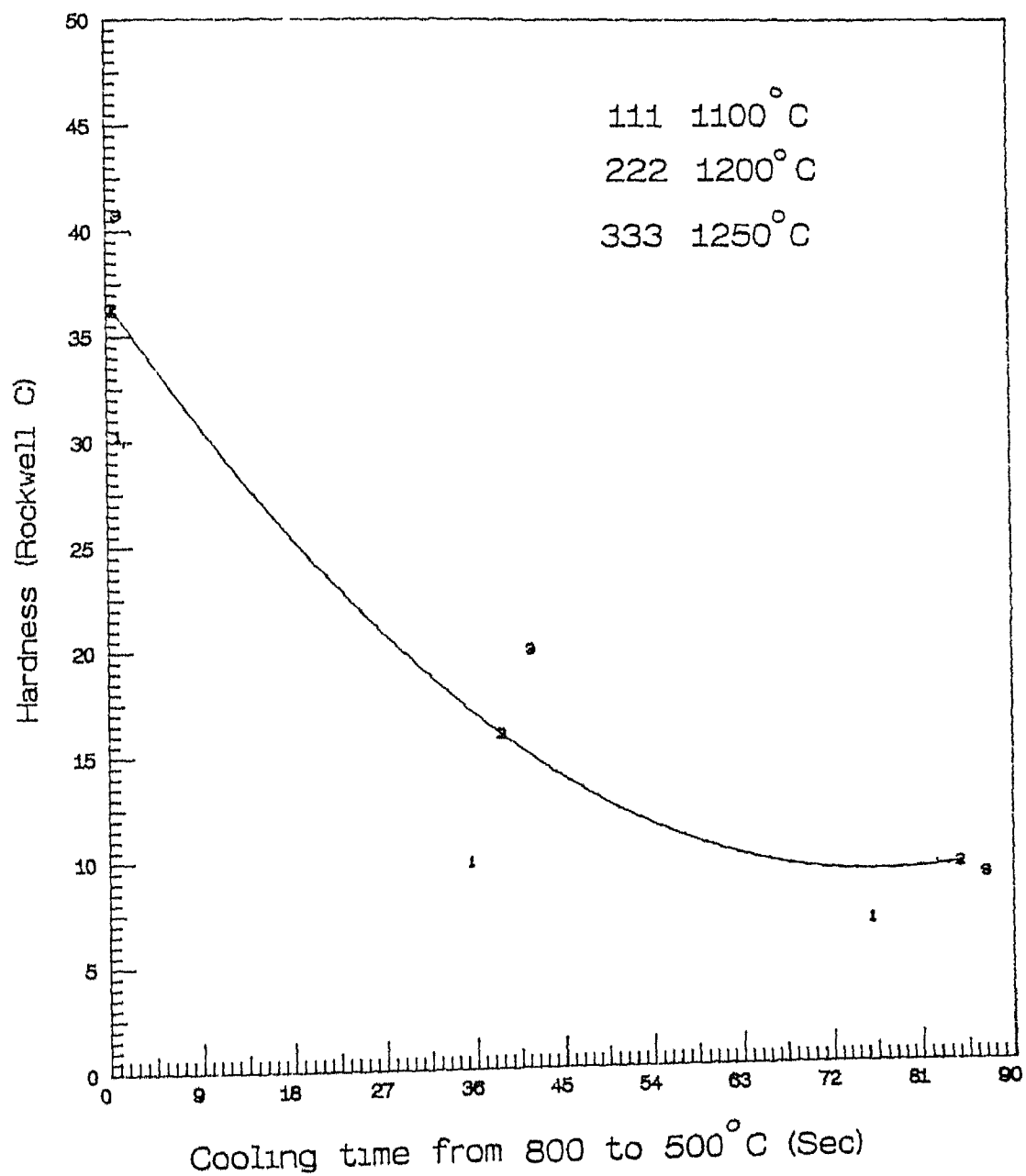
Fig 6 2   Hardness vs t_{8-5} for simulated steel A

58

Reported data on solubilities of carbides and nitrides of some elements of interests are plotted in Fig 6 3 [4] At high cooling rate, reprecipitation of carbides and nitrides might not occur at the equilibrium transformation temperatures At lower temperatures of 400 to 600°C, carbide and nitrides particles may be produced in fine dispersed form This adds to strength and hardness to the materials Samples which were air cooled get sufficeint time for reprecipitation of carbides and nitrides, which lowers the hardness Schematic representation of metallurgical changes occuring at different peak temperatures and cooling rates are shown in Fig 6 4 It is not always feasible to identify these phases in optical microscope Careful examinaion of the material at very high magnification using scanning electron microscope and transmission electron microscope might help in better evaluation of data

Results of toughness measurements using charpy impact testing of weld simulated samples show that toughness is maximum when samples were forced air cooled insteat of being water quenched or annealed Thoughness of metal is related to absorption of energy before fracture and depends on both strength and ductility With water quenching of steel samples, hard and strong martensite phase is formed having very poor ductility Toughness of the water queched weld simulated sample is therefore low Similarly for annealed samples, ductility is high but tensile strength is low Air cooled samples have the best combination Results carried out for simulated samples of steel of type-A at room temperature and those of type-C at 0°C agree well with those

Figure C 3 Solubility products of carbides and nitrides in austenite as a function of temperature After Aaronson B *Steel Strengthening Mechanisms* Clim Molybdenum Co 1969
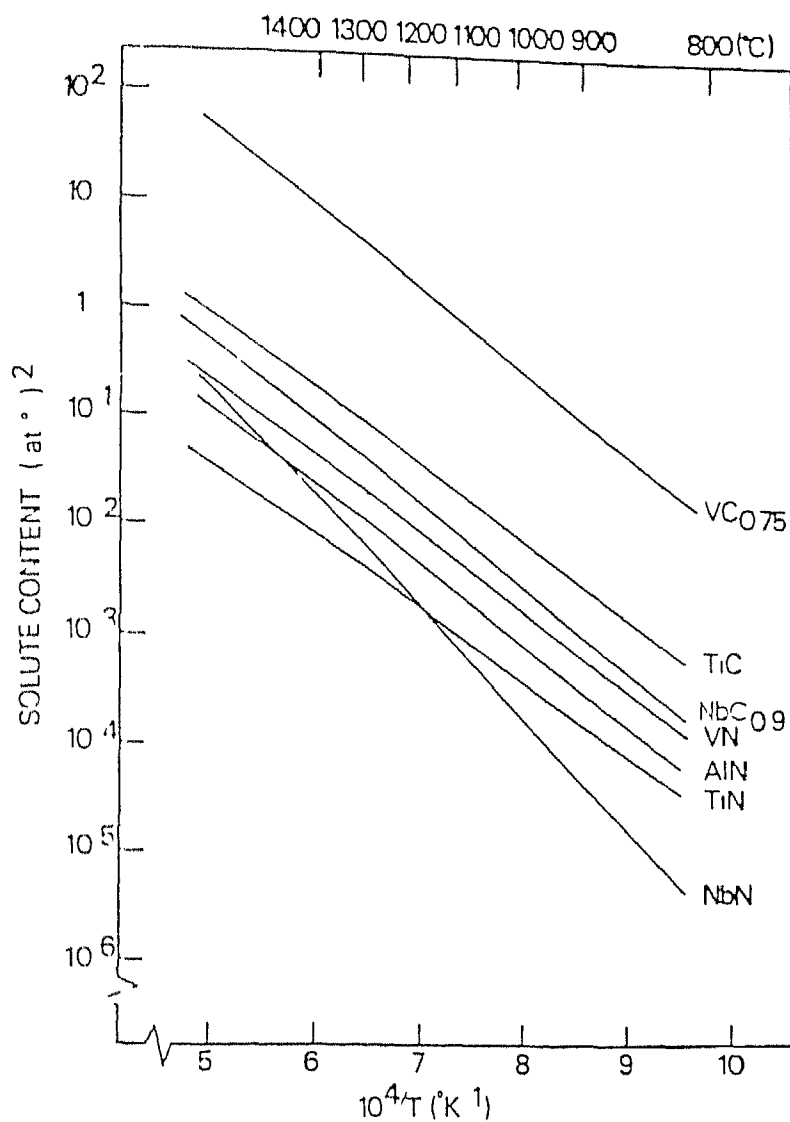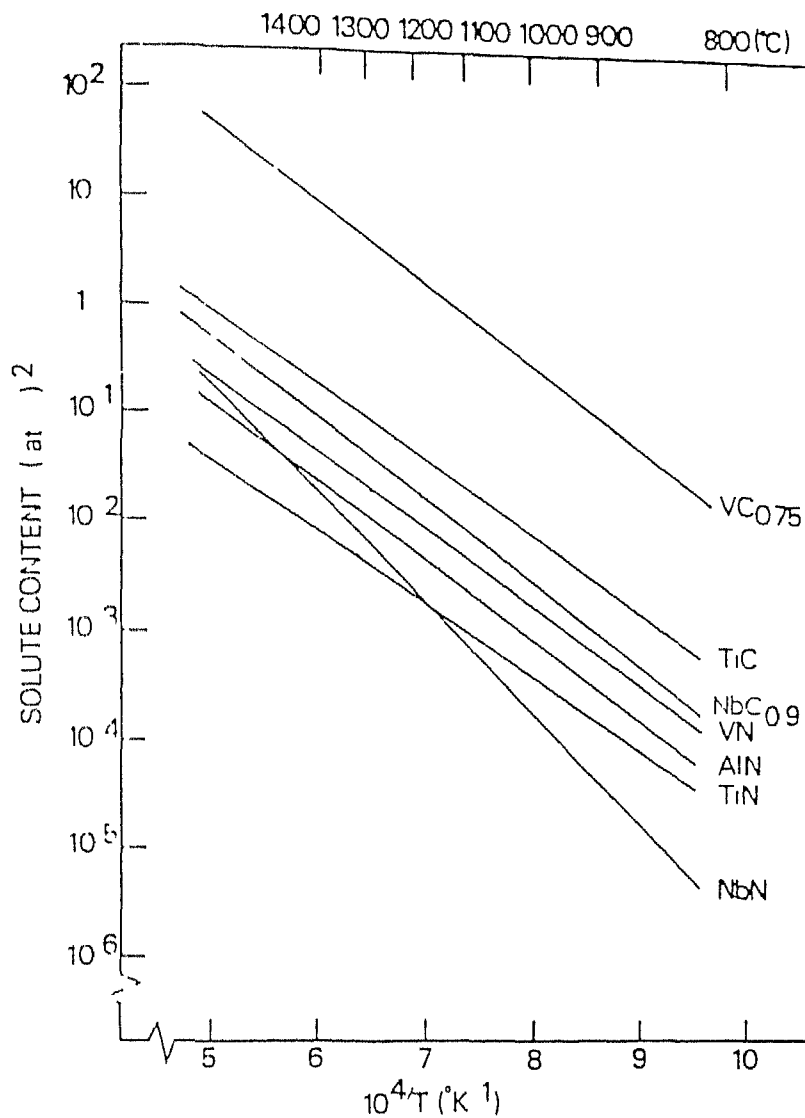
Figure 6.3 Solubility products of carbides and nitrides in austenite as a function of temperature. After Aaronson, B, *Steel Strengthening Mechanisms*, Climax Molybdenum Co, 1969

CHAPTER SEVEN

7   SUMMARY AND CONCLUSIONS

The weldability of different kinds of Nb-microalloyed HSLA steels has been evaluated by studying the microstructural changes and mechanical properties of simulated samples which correspond to various regions in the heat affected zone of weldments   For this the tensile and impact test samples were rapidly heated to certain peak temperature in the range of 1100 - 1250°C and then allowed to cool on a predetermined manner to obtained varying severity of quenched   The following conclusions may be drawn from the results of the present study

1   The maximum hardness was obtained when the sample was heated to a peak temperature of 1250°C and water quenched   This is attributed to the increased hardenability of steel due to grain growth of the austenite phase and dissolution of carbides and nitrides of elements such as niobium   Lower temperature transformation products such as martensite and bainite are formed in these weld simulated test samples   Such samples have elongation to failure of ~ 7 pct   An elongation of 27 55 pct   was observed on the samples which were allowed to cool in air   The brittle and ductile behaviour of weld simulated test samples has been well supported by the

fractographic studies of the surface after the tensile testing Ductility of the sample was well represented by the existance of dimples in fractographs and also by elongation of grains in the direction of applied force in many cases

2   Toughness of steel was measured by the standard charpy impact testing method Best results were obtained when steel samples were cooled in air compared to water quenched or annealed samples Toughness tends to reflects the combination of both strength and ductility of the materials

3   Results of weld simulated tensile and impact test samples may be used to evaluate the weldability of steel under a given set of operating conditions such as plate thickness, weld velocity, heat input and the preheat temperature of the plate The present results show that Nb microalloyed steel could be welded without inducing detrimental hard and brittle martensite phase in the heat affected zone in most cases of interest

REFERENCES

1   Cornu, Jean "Advanced Welding Systems", Vol 1, pp 12

2   Tanaka, Tomo "Overview of High Strength Steel", Transaction
     of Indian Institute of Metals, 49(3), pp 101-112,June(1996)

3   Hrivnak, I The Mutual Relationship and Interdependence of
     Developments in Steel Metallurgy and Welding Technology,
     Welding in the world, 16 1 1978

4   Easterling, K E , "Introduction to Physical Metallurgy of
     Welding" Butterworth and Company London, England, (1983)

5   Collins, L E, Goddens, M J and Boyd, J D Microstructure in
     line pipe steels, Canadian Metallurgical Quarterly   22(2),
     pp 169-179, (1983)

6   Rosenthal, D Welding Journal, 20(5), 229-S to 234-S (1941)

7   Pavelic, H , Tanbakuchi, R , Uyehara, O A , and Myers, P S ,
     Welding Journal, 48, 295-S to 305-S (1969)

8   Papazoglou, J , Masubuchi, K , Goncalves, E , and Imakita,A ,
     ASME, 12 (1982)

9   Goldak, J , Bibby, M , Moore, J and Patel, B , Met   Trans
     17B, pp 587 - 600, (1986)

10   Patro, A K , M Tech Project entitled "Numerical Modelling
     and Weld Simulation of HSLA Steel", IIT, Kanpur, June (1996)

11   Nippes, E F and Savaga, W F , "Development of specimen
     simuliting weld heat affected zone", Welding Journal, 28(11),
     534-S to 546-S, (1949)

12 Kabayashı, H , "Decomposıtıon process of M-A phase ın HAZ of high strength steel", Canadıan Metallurgıcal Quarterly,23(3), pp 333 - 339, (1984)

13 Bowker, J T , Ng-Yelım, J and Malıs, T F , "Effect of weld thermal cycle on behavıour of Tı-Nb carbonıtrıdes ın HSLA steel", Materıals Scıence and Technology, 5(10), pp 1034 - 1036, (1989)

14 Godden, M J and McGrath, J T , "The assessment of HAZ toughness of lıne pıpe steels", Canadıan Metallurgıcal Quarterly, 20(4), pp 449 - 451 (1981)

15 Faırchıld, D P , Banguru, N V , Koo, J Y , Harrıson, L P and Ozekcına, Weldıng Journal, 70(12), pp 321-S - 329-S, (1991)

16 Hougardy, H P , steel "A Hand Book of Materıals Research and Engıneerıng",Vol 1,Sprınger-Verlag,Berlın,pp 504-534, (1992)

17 Harrıson, P L and Farrar, R A , Int Materıals Research , 34(1), pp 35 - 51, (1989)

18 Brownrıgg, M J and Boelen, K M ,"Internatıonal Conference on HSLA steel Technology and Applıcatıons", ASTM, Phıladelphıa USA, (1984)

19 Gıanetto, J A , Smıth, N J , McGrath, J T , and Bowker, J T , "Effect of Composıtıon and Energy Input on Structure and Propertıes of Hıgh Strength Metals", Weldıng Journal, Vol 71, No 11, (1992)

20 Aaronson, B , Steel Strengthenıng Mechanısms, Clımax Molybdenum Co , (1969)

21 Dıeter, G E , "Mechanıcal Metallurgy", pp 538

22 Metal Hand Book (Amerıcan Socıety for Metals), vol 7

MME-1596 - M -SAR-MEC